Parameter identification for a runoff model
for forest roads

Charles H. Luce

Intermountain Research Station, U.S. Department of Agriculture Forest Service, Moscow, Idaho

Terrance W. Cundy

College of Forest Resources, University of Washington, Seattle

Abstract. Rainfall simulation is a commonly used approach for studying runoff and
erosion from forest roads, and a method is needed to estimate infiltration parameters
from these experiments. We used two algorithms, the Simplex and Shuffled Complex
Evolution, to estimate parameters for a physically based infiltration and overland flow
model. Each algorithm was tested by estimating parameters for 92 field-measured
hydrographs from forest roads. Nine of the field-measured hydrographs allowed us to
further test whether estimated parameters could be extended to other antecedent
conditions and plot sizes. The results demonstrate (1) the physically based model is
able to estimate hydrographs from forest roads, (2) the two algorithms find unique
parameter sets in spite of an error surface that suggests identifiability problems
between the hydraulic conductivity and pressure parameters, (3) the two algorithms
converged to the same parameter values, and (4) that parameters estimated for one
antecedent condition and plot size can be extended to others with reasonably small
error.

Introduction

Dirt roads built to access forest lands are major and
persistent sources of sediment to headwater streams. Public
and private landowners are increasingly being required to
evaluate sediment contributions from both existing and
proposed roads as part of environmental analyses to protect
fish and water resources. To improve predictions of sedi-
ment production from forest roads, the U.S. Department of
Agriculture Forest Service is building a forest road compo-
nent for the Water Erosion Prediction Project [Burroughs et
al., 1991], a physically based model of hydrology and
erosion.

Accurate infiltration parameter estimates are needed to
drive the model. Rawls et al. [1989] developed methods to
estimate Green-Ampt infiltration parameters for croplands
and rangelands, but their empirical formulas are inappropri-
ate for coarse-grained soils common to road surfaces and to
compacted conditions. Estimates of infiltration capacity for
roads have been made by several authors. Reid and Dunne
[1984] measured runoff from roads during natural rainfall
events. They found the steady state infiltration rate averaged
over the complete road profile by subtracting the runoff rate
from the rainfall rate during periods of uniform rain inten-
sity. While the infiltration rates they found were small, they
were high enough to prevent runoff for several rainfall
events.

Rainfall simulation is commonly used to measure infiltra-
tion and overland flow on roads and has the advantages of
providing control of rainfall timing and intensity, sampling
over a relatively large area, and measuring in situ with

minimal disturbance of the sampled area. Ward and Sieger
[1983], Ward [1986], and Flerchinger and Watts [1987] used
a least squares fit of the infiltration rate to the reciprocal of
the accumulated infiltrated depth to determine values for the
Green-Ampt infiltration parameters from rainfall simulation
data. Ward [1986] was dissatisfied with this method because
it frequently yielded negative parameter values. Ward and
Bolin [1989a, b] and Ward and Bolton [1991] used the
regression approach or an average of the final three steady
state infiltration rates from a simulated event to estimate the
hydraulic conductivity; they then back-calculated the suc-
tion head using the hydraulic conductivity estimate and total
depth of infiltration for the simulated event. These methods
occasionally yielded physically impossible parameters, and
the authors found it necessary to resort to trial and error in
those instances.

To properly use rainfall simulator data for parameter
estimation, infiltration information must be extracted from
the hydrograph. None of the previously discussed studies
explicitly consider routing in their methods to estimate
infiltration parameters. In this paper, we test two algorithms
to estimate infiltration parameters from hydrographs ob-
tained using rainfall simulation. Estimated parameters are
used in a physically based model of Horton overland flow,
including infiltration, depression storage, and routing, to
predict the hydrograph.

The major issues to be investigated are as follows: (1) to
see if the physically based model of Horton overland flow
can reproduce hydrographs with physically meaningful pa-
rameter sets, (2) to determine whether the estimation algo-
rithms yield unique parameter sets, and (3) to see if param-
eters estimated for a given set of conditions are applicable to
other antecedent conditions and plot sizes.

Table 1. Information About Locations and Soils Where Rainfall Simulation Was Done

Location	Parent Material	Texture	Year
Deep Creek, Idaho	metamorphic-gneiss	sandy silt	1989
Hahn's Peak, Colorado	eolian sandstone	fine sandy loam	1989
Park Lake, Montana	metamorphic-schist	sandy silt loam	1988
Potlatch River, Idaho	loess	silt loam	1990
Tin Cup Creek, Idaho	metamorphic-shale	silt clay	1989
Tea Meadow, Idaho	loess	silt loam	1990

Methods

Field Data Collection

Rainfall simulations were performed on forest roads on six different soils. Descriptions of the soils are in Table 1. More than one road segment was used for simulation on some soils, yielding 11 sites. Information for each site is listed in Table 2. Each site had three plots, two 1-m wide by 1-m long plots and one 1-m wide by 5-m long plot, except for the site at Park Lake, which had only two 1-m by 1-m plots and no 1-m by 5-m plot. This yielded a total of 32 plots. An example layout from the Tea Meadow Site is presented in Figure 1. Each plot was subjected to three rainfall events, giving a total of 96 hydrographs. Three hydrographs from Potlatch River were discarded because the pump gradually ceased operation during the final event, and one hydrograph from Hahn's Peak was discarded because of a bad nozzle over one of the plots for one event. The remaining 92 hydrographs were used in the analysis.

Plots were installed on native surfaced forest roads freshly bladed to remove ruts and form a smooth, uniform surface. Sidewalls made of sheet metal were installed parallel to the direction of flow and sealed to the road surface with latex and bentonite. Headwalls with covers were set up at the bottom to collect runoff.

Three 30-min rainfall events were simulated at each site. The first event, designated the "dry" event, occurred with soil moisture at the condition found when arriving at the site; the second event, designated "wet," was 24 hours later; and the third event, designated "very wet," occurred as quickly after the second as possible, usually about 30 min.

Rainfall was applied with an oscillating rainfall simulator (modified Purdue). A windscreen surrounded the plot. Rain-

fall intensity was measured before and after each event using metal pans covering each plot. Rainfall was set to a nominal intensity of either 30 mm/h or 50 mm/h, and only one nominal intensity was used at a site. The nominal intensity for each site is listed in Table 2. A reasonably constant intensity was maintained with a flow regulator, although there was a decrease of head in the feeding tank. For the Hahn's Peak data, which were typical of all of the data, the coefficient of variation of rainfall intensity calculated from the before and after measurements averaged 0.7% and never exceeded 1.4%. Spatially, the rainfall varied little as well. For the Hahn's peak data, the coefficient of variation for rainfall intensity between three plots averaged 3.4% for six events and never exceeded 4.6%.

Runoff was measured differently in the 3 years of study. In 1988 when the Park Lake site was studied, runoff was measured in the field directly in graduated cylinders hooked to a bubble gauge to record the level every 20 s. In 1989 and 1990, grab samples lasting 30 s were collected every 45 s. If the 1-L sample bottle was close to filling before 30 s, it was removed. Exact time of collection was measured on a stop watch, and flow rate was calculated by dividing volume collected by time. Volumes of one half of the samples were determined in the laboratory gravimetrically; volumes of the other half were determined from measurements in the field. In 1989 volumes of field-measured samples were measured in graduated cylinders, and in 1990 volumes of field-measured samples were measured on scales. A correction factor determined in the laboratory was applied to the field-measured samples to account for their sediment content.

Antecedent conditions were determined by soil moisture content. Volumetric moisture content was calculated from

Table 2. Topographic and Rainfall Information About Specific Sites

| Site	Surface D_{50}, mm	Nominal Rain Intensity, mm/h	Slope, %		
			Plot 1	Plot 2	Plot 3
Deep Creek 1	2.08	30	5.7	6.5	6.6
Deep Creek 2	2.08	50	5.9	6.9	6.2
Deep Creek 3	1.72	30	1.8	3.6	4.2
Hahn's Peak 1	0.23	30	8.8	10.2	8.7
Hahn's Peak 2	0.23	50	4.7	4.6	4.4
Hahn's Peak 4	0.13	50	6.4	6.5	7.1
Park Lake 1	0.76	30	n/a	6.3	5.3
Potlatch River 3	0.09	50	5.1	5.0	4.9
Tin Cup Creek 1	0.20	30	8.5	9.6	7.7
Tin Cup Creek 2	0.20	50	13.5	14.4	11.8
Tea Meadow 5	0.03	50	6.5	6.5	7.3
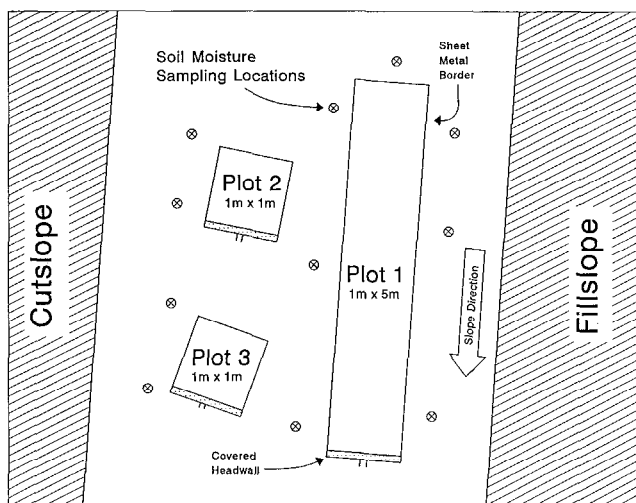
Figure 1. Example layout of a site for rainfall simulation showing the three plots.

the average moisture content, mass basis, of the points closest to each plot (Figure 1) multiplied by the specific gravity of the soil measured in that plot. To ensure that the plot and soil moisture sampling sites received the same amount of rainfall, locations where soil moisture samples were taken were covered at the beginning and end of each event at the same time that the plots were covered for measuring rainfall intensity. Bulk density was measured within the plots after the third event by the compliant cavity method [*Grossman and Pringle*, 1987].

While a large data set from many sites was available for parameter estimation, we used only the data from one of the sites, Tea Meadow, for testing the parameters on different plot sizes and antecedent conditions. Data collected at the other sites were inadequate for the test. Prior to 1990, soil moisture contents were not measured such that the moisture content of the plots at the beginning of each event were accurate. Although the Potlatch River site was also measured in 1990, the rainfall simulations were done after two weeks of wet weather in the snowmelt season, and the site was nearly saturated for all events. This meant that we could not test how well we could extend the results to other antecedent conditions. In addition, the pump failed during the final event, so only a portion of the data were useful.

Modeling Approach

The overland flow model assumes the case of Horton overland flow, where runoff is generated only when rainfall intensity exceeds infiltration capacity. It is a semianalytic solution to the kinematic wave overland flow equation using Philip's infiltration equation to calculate rainfall excess for the case of constant rainfall intensity [*Cundy and Tento*, 1985; *Luce and Cundy*, 1992]. The model uses four parameters to model the processes of infiltration, depression storage, and overland flow.

Infiltration is given by the model of *Philip* [1969] modified for constant intensity rainfall [*Cundy and Tento*, 1985]:

$$f(t) = A + B[t - (t_p - t_s)]^{-1/2} \quad (1)$$

where t is time from the onset of rain (T), $(f(t)$ is the infiltration capacity at time $t(L/T)$, A is the conductivity

(L/T), and B is the sorptivity at the initial soil moisture content $(L/T^{1/2})$. The factor $t_p - t_s$ is a time correction composed of the actual time to ponding (t_p) and the time when $f(t) = i$ under a continuously ponded condition (t_s), where i is the constant rainfall intensity (L/T).

Depression storage $h_n(L)$ is the maximum equivalent depth of water that can be stored on the surface before flow will begin. If the depth of depression storage is known, then the time at which it is filled and runoff begins $t_n(T)$ can be found from

$$h_n = \int_{t_p}^{t_n} i - f(t)\, dt \quad (2)$$

substituting the relationship for $f(t)$ described by (1) gives

$$h_n = (i - A)(t_n - t_p) - 2B(t_n - t_p + t_s)^{1/2} + 2Bt_s^{1/2} \quad (3)$$

where t_n can be found numerically.

Overland flow is modeled using the kinematic wave approximation

$$\alpha \beta h^{\beta-1} \frac{\partial h}{\partial x} + \frac{\partial h}{\partial t} = i - f(t) \quad (4)$$

where h is the flow depth (L), x is the distance downslope (L), and α and β describe the stage discharge relationship

$$q = \alpha h^\beta \quad (5)$$

where q is the discharge per unit width (L^2/T). In the case of overland flow on forest roads, flow lengths are sufficiently short that for the rainfall intensities used here, a laminar regime was thought to represent the overland flow best. Runoff from the plots had Reynolds numbers of the order of 10; therefore α and β are given by

$$\alpha = gS_0/k\nu \quad \beta = 3 \quad (6)$$

where g is gravitational acceleration (L/T^2), S_0 is bed slope (L/L), ν is kinematic viscosity (L^2/T), and k is a dimensionless roughness coefficient.

Both the kinematic wave and Philip's equations are approximations to the true field situation. A principal assumption for this model is that there is no spatial variation in soil or hydraulic properties. Freshly bladed road surfaces are almost ideal for testing this model, as they come close to meeting this assumption. A further assumption in Philip's model is that initial soil moisture does not vary with depth. No measurements were taken to confirm the validity of this assumption.

Parameter Estimation Algorithms

In general, a four-parameter problem is posed, with the objective of finding the best A, B, h_n, and k parameter set to reproduce a given field hydrograph. In this analysis, k was estimated independently following the method of *Katz* [1990]; he investigated surface roughness in laboratory experiments on artificial road surfaces and found a relationship between k, median soil aggregate diameter, and rainfall intensity

$$k = 25.17 + \left(\frac{D_{50}}{.7}\right)^{4.87} + \left(\frac{i}{40}\right)^{3.39} \quad (7)$$

where D_{50} is median soil aggregate diameter in millimeters and i is rainfall intensity in millimeters per hour. When D_{50}
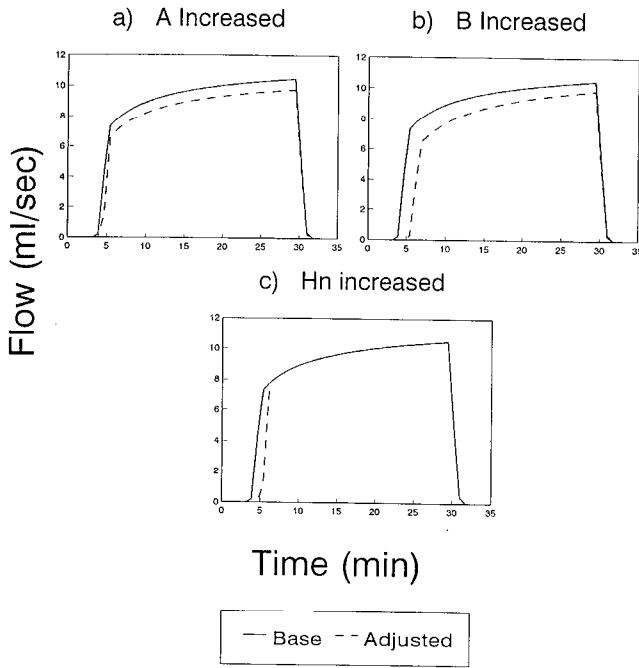
Figure 2. Hydrographs showing effects of changes in three parameters in the kinematic wave–Philip infiltration overland flow model: (a) increase in A, (b) increase in B, and (c) increase in h_n.

is less than 0.7 mm it is set equal to 0.7 mm, and when i is less than 40 mm/h, it is set equal to 40 mm/h.

The following brief sensitivity analysis will show how changes in the remaining three parameters, A, B, and h_n, affect the hydrograph. The analysis illustrates potential problems in arriving at unique estimates of A and B. For the following examples, we used $A = 5.0$ mm/h, $B = 5.0$ mm/h$^{1/2}$, $D_{50} = 1.69$ mm, $h_n = 0.5$ mm, $S_0 = 0.05$, a plot length L of 1 m, and a 30-min rainfall at $i = 50$ mm/h.

Figure 2a shows hydrographs with $A = 5.0$ mm/h (the base case) and $A = 7.5$ mm/h, an increase of 50%. There are three distinct effects of increasing A: (1) the time to ponding increases, (2) the time to fill depression storage increases, and (3) the peak flow rate decreases.

Figure 2b shows hydrographs with $B = 5.0$ mm/h$^{1/2}$ (the base case) and $B = 6.5$ mm/h$^{1/2}$, an increase of 30%. Qualitatively, the effects of increasing B are similar to those of increasing A. However, the delay in runoff is greater, and there is an increase in curvature, concave down, of the upper limb of the hydrograph.

Figure 2c shows hydrographs with two different values of h_n: $h_n = 0.5$ mm (the base case) and $h_n = 1.0$ mm, an increase of 100%. An increase in h_n causes a delay in initiation of runoff and a very slight steepening of the rising limb. There is no effect after the time of concentration (the time when the rising limb of the hydrograph changes from concave up to concave down). Because of the steepness of the rising limb, small errors in timing can have a large effect on any error function which uses differences between observed and predicted hydrographs. Therefore when trying to estimate at A and B, it is necessary to allow h_n to vary so that the estimate of h_n does not unduly affect estimates of A and B.

A and B have similar effects on the runoff hydrograph, potentially creating an identification problem. Figure 3 shows an error surface for the hydrograph we used in Figure 2, calculated as the mean-squared differences between the predicted and base case hydrographs, plotted above the A-B plane to show how joint variations in A and B affect the error value. The prominent feature in the error surface is the trough angled between A_{min}, B_{max} and A_{max}, B_{min}. The trough identifies a region where the effects of high and low values of A are offset by low and high values for B, respectively. Figure 4 shows the base-case hydrograph plotted with predicted hydrographs from two A,B pairs with similar errors of about 4.7×10^{-6}. One predicted hydrograph used $A = 8.75$ mm/h, an increase of 75%, and $B = 3.75$ mm/h$^{1/2}$, a decrease of 25%. The other hydrograph used $A = 2.5$ mm/h, a decrease of 50%, and $B = 6.0$ mm/h$^{1/2}$, an increase of 20%. Depression storage h_n was adjusted to 0.9 mm for the first hydrograph and 0.17 mm for the second so that the rising limb did not unduly influence the error values. The systematic errors in the predicted hydrographs are visually apparent, but they do not greatly affect the overall sum of squared differences. This highlights the potential for nonunique parameter sets based on error function evaluation. We therefore tried two algorithms, one that has been demonstrated to find the global minimum and another, more traditional, approach that is more susceptible to identification problems.

The objective function used was a simple mean-squared differences

$$\text{Err} = (1/n) \sum_{1}^{n} (q_p - q_0)^2 \qquad (8)$$

where n is the number of discharge observations, q_p is the predicted flow (L^3/T), and q_0 is the observed flow (L^3/T). The model predicts only instantaneous flows, so the predicted flows q_p are the average of the instantaneous flow predicted at the observation time and 15 s before and 15 s
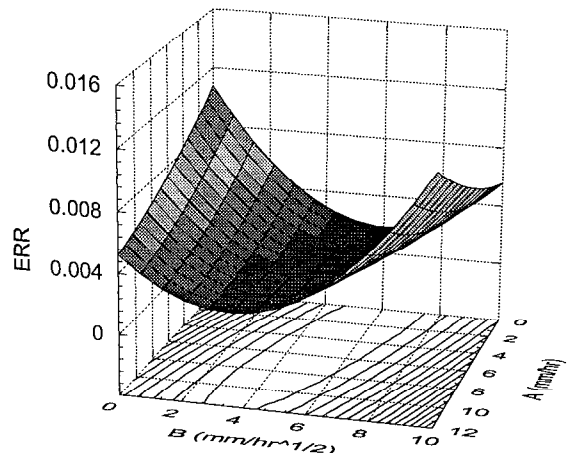

Figure 3. Error surface in A-B plane with h_n fixed at true value (0.5 mm). Contours on bottom show that the trough has little relief from end to end. Error surface is zero at $A = 5$ mm/h and $B = 5$ mm/h$^{1/2}$.
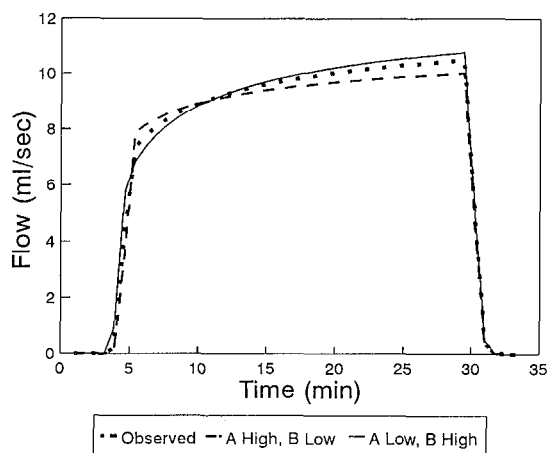
Figure 4. Hydrographs showing systematic errors from A overpredicted–B underpredicted and A underpredicted–B overpredicted combinations. Both predicted curves have about the same error value.

after. This averaging is consistent with the field measurement methods discussed earlier.

Luce [1990] used a grid search method to estimate A, B, and k. The method was time consuming and generated multiple parameter sets that subsequently had to be sorted subjectively. In this analysis, we tried two different automated methods to estimate a unique parameter set for each hydrograph. The first method was the Simplex method described by *Nelder and Mead* [1965]. We used the code from *Press et al.* [1986] for this specific application with a single start. This method is fast but can converge at a local minimum if the error surface is flat or pitted. The second method was the Shuffled Complex Evolution (SCE) described by *Duan et al.* [1992]. This method was developed to find the global optimum for error surfaces that potentially could have many local minima.

The Simplex method searches through the parameter space using a tetrahedron (4 points in this case) to find the minimum error value. An initial tetrahedron is set up using four of the eight corners of the search space of reasonable parameter values. A new tetrahedron is formed by replacing the point on the tetrahedron having the greatest error with a point with lower error. This new point is generated either by reflecting the worst point through the centroid of the other three points or contracting it toward the centroid. If neither of these approaches finds a point with lower error, the entire tetrahedron is contracted towards the point having the lowest error. The process is iterated until convergence is found.

The SCE method essentially uses multiple Simplex tetrahedrons whose points are periodically shuffled to avoid the possibility that the method will settle outside of the global optimum. For our application, 49 initial points, randomly selected from within the search space, are sorted into 7 complexes each containing 7 points. Four points are selected randomly from a complex to form a tetrahedron. The point with the greatest error value in the tetrahedron is replaced by a point with less error using two iterations of the Simplex method as described in the preceding paragraph, after which the tetrahedron is dissolved and the updated points are returned to the complex. Four new points are selected randomly

from the updated complex to form a new tetrahedron. This process of randomly forming a tetrahedron and iterating through the Simplex method is performed 7 times for each of the 7 complexes, after which 7 new complexes are formed from the updated points in a shuffling (not random) action. This process is repeated until convergence is reached.

A search space of reasonable parameter values is required for both methods. The SCE method explicitly requires a parameter space in which to work, and the Simplex method may attempt to search outside of reasonable ranges. We allowed the Simplex method to look outside of the reasonable ranges, but set the error function for parameter values outside of the bounds at 5×10^9, which is much greater than the error value that could be calculated from a hydrograph. This effectively forced the Simplex method to search within the space of physically reasonable parameter values.

The maximum value of A that could be expected would be the rainfall intensity minus the highest observed flow rate converted to a unit area basis, and was set as

$$A_{max} = i - 0.9(q_{max}/L) \qquad (9)$$

where q_{max} is the maximum observed flow per unit width (L^2/T), and L is the plot length. The 0.9 factor was added because there were fluctuations in observation of peak flow that could lead to an observed peak flow greater than the conductivity and rainfall would allow. The minimum value of A was set to 0.

We used observations of the beginning of runoff to set the maximum value of B. The time that runoff is first observed t_{n0} must occur after t_p, and can be considered a maximum estimate of t_p. Time to ponding under constant rainfall can be calculated using Philip's equation

$$t_p = \frac{A\left(\frac{B}{(i-A)}\right)^2 + 2\left(\frac{B^2}{(i-A)}\right)}{i} \qquad A < i \qquad (10)$$

and because both A and B both act to increase t_p, we can use $A = 0$ to find the maximum possible value of B as

$$B_{max} = \frac{it_{n0}^{1/2}}{\sqrt{2}} \qquad (11)$$

B has a minimum value of 0. A further condition on B is that if $A = 0$, then $B = 0$.

Depression storage was constrained between 0 and 20 mm. A depth of 0 mm is the physical minimum, and field observations suggested that more than 20 mm of depression storage on the freshly graded forest road plots was implausible.

The four points used to start the Simplex method were $(A, B, h_n) = (0, 0, 0)$, $(A_{max}/5, 0, 0)$, $(A_{max}/5, B_{max}/5, 0)$, $(0, 0, h_{nmax}/10)$. Convergence for the Simplex method was based on the difference between the minimum and maximum values, which was compared to a fraction ε of the average of the minimum and maximum error values. In the analysis here, ε was set to 1×10^{-6}. This tolerance was found by using 1×10^{-3} for initial tests and decreasing the tolerance by an order of magnitude until it no longer converged reliably at 1×10^{-7}.

The SCE was started with 49 randomly selected points within the search space, sorted into 7 complexes each

Table 3.   Descriptive Statistics of Errors From the Two Fitting Methods for All 92 Hydrographs

	Simplex Method					SCE Method				
Statistic	Mean-Square-Error	% Error Volume	% Error Peak Flow	Absolute Value % Error Volume	Absolute Value % Error Peak Flow	Mean-Square-Error	% Error Volume	% Error Peak Flow	Absolute Value % Error Volume	Absolute Value % Error Peak Flow
Mean	0.00202	−1.171	0.050	1.431	2.324	0.00197	−1.026	0.152	1.111	2.045
Median	0.00104	−0.561	0.628	0.740	1.605	0.00095	−0.507	0.701	0.546	1.472
Minimum	0.00029	−11.663	−16.912	0.044	0.002	0.00028	−8.258	−15.650	0.001	0.002
Maximum	0.01084	4.318	9.202	11.663	16.912	0.00954	0.912	8.173	8.258	15.650
Standard deviation	0.00205	2.202	3.628	2.041	2.776	0.00198	1.544	2.998	1.483	2.188

Mean square error is calculated by (8), percentage error in volume is calculated by (15), and percentage error in peak flow is calculated by (16).

containing 7 points. We determined convergence for the SCE approach when the range between the A, B, and h_n values of the best 5 points was 1×10^{-3} times the range of the original search space. We started with a tolerance of 0.1 and decreased it by an order of magnitude until convergence was no longer reliable at 1×10^{-4}. Our convergence criterion was different than that of *Duan et al.* [1992] because they were fitting model outputs and determined convergence when the error was within a tolerance limit of zero error. This also was a different convergence criterion than for the Simplex method. While the Simplex method checks to see if the points are similar in error value, the SCE criterion checks to see if they are close in space.

As an example of the resources required, the Simplex method took about 5 min, and the SCE method took about 3 hours to obtain parameter values for the hydrographs shown in Figure 2. Both were compiled BASIC programs run on a 33-MHz 386 computer.

Predicting Hydrographs for Changes in Antecedent Condition and Plot Size

The plots at Tea Meadow were used to see if parameters estimated for a given set of conditions are applicable to other antecedent conditions and plot sizes. We adjusted the SCE parameter sets from the wet event on the three plots to predict all of the other event-plot combinations at Tea Meadow. For example we used the parameter set from the wet event on plot 1 to predict the hydrographs for the dry and very wet events on plot one and the dry, wet, and very wet events on plots 2 and 3.

In order to predict runoff for different antecedent conditions, it is necessary to know the how the parameters change for the new antecedent conditions. Of the four parameters A, B, h_n, and k, we adjusted only B. *Philip* [1990] suggested that the ratio A/K_s, where K_s is the saturated hydraulic conductivity (L/T), changed with initial soil moisture content $\theta_i(L^3/L^3)$, with $A/K_s = 1$ at $\theta_i = \theta_s$, and $A/K_s < 1$ for $\theta_i < \theta_s$, where $\theta_s(L^3/L^3)$ is the saturated soil moisture content. He showed that the ratio for a Yolo light clay varied from 0.4 for dry conditions to 1.0 for saturated conditions, which is probably less than A varies from point to point on even a relatively homogeneous road. In any event, we did not have the data required by Philip with which to predict the changes in A with moisture content. Presumably, depression storage h_n and roughness k would change with the sequence of events, since erosion processes remove some roughness

and depression features and create others. Exactly how they would change, or even the direction of change, is not clear.

The sorptivity parameter in Philip's equation B is a function of the initial soil moisture content. Using *Fok* [1975] and *Campbell* [1974], B can be estimated from

$$B = \left((\theta_s - \theta_i) A \Psi_s \frac{2b + 3}{b + 3} \right)^{1/2} \qquad (12)$$

where θ_s and θ_i are the saturated and initial volumetric soil moisture contents (L^3/L^3), Ψ_s is the bubbling pressure, and b is the slope of the log (Ψ) versus log (θ/θ_s) plot. For a given soil, Ψ_s, A, b, and θ_s can be considered constant and grouped into one constant, C, and we can write

$$B = C((\theta_s - \theta_i))^{1/2} \qquad (13)$$

So the B value for any other antecedent moisture content B_p can be determined from the initial estimate of B, B_0, and the square root of the ratio of the soil moisture deficits:

$$B_p = B_0 \left(\frac{(\theta_s - \theta_i)_p}{(\theta_s - \theta_i)_0} \right)^{1/2} \qquad (14)$$

We used the parameters estimated for the wet event by SCE for all predictions. The A and h_n values were unchanged, and B was adjusted for the dry and very wet initial conditions as described above.

Percentage Error Calculations for Field Hydrographs

In preparing the results, we developed two normalized measures of error. We could not normalize the data based on mean square error as given in (8), because hydrographs from very wet conditions consistently had a lower total sum of squares than did the dry events. The reason for this is that the hydrographs for the very wet event rose to the equilibrium limb sooner, and the mean was closer to the equilibrium limb, where most of the observations were made. We used percentage error in volume and peak flow as measures of accuracy. The three indices mean square error, error in volume, and error in peak flow define the important aspects of the hydrographs.

We calculated percent error in volume E_V as
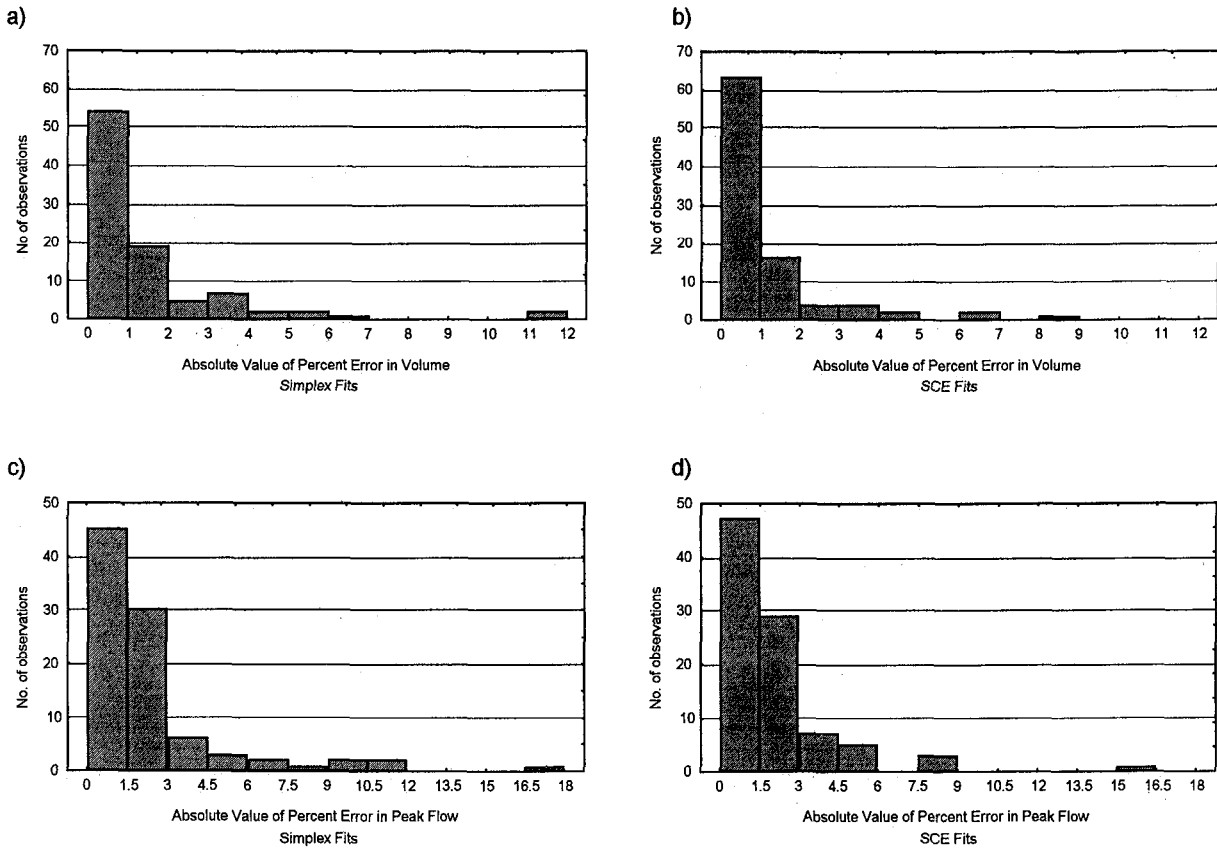
$$E_V = \frac{V_m - V_0}{V_0} \qquad (15)$$

Figure 5. Histograms of the absolute value of percent error for (a) volume for simplex method, (b) volume for SCE method, (c) peak flow for simplex method, and (d) peak flow for SCE method.

where V_m is the modeled volume, and V_0 is the observed volume. Volume was calculated as the time integral of the hydrograph using a trapezoidal rule.

Percentage error in peak flow E_P was calculated by

$$E_P = \frac{P_m - P_0}{P_0} \qquad (16)$$

Figure 6. An example of a well-fitted hydrograph, Tin Cup Creek 1, plot 3, wet event. Least square error is 0.00055 (mL/s)^2, percent volume error is 1.14%, and percent peak error is −0.51%.

where P_m is the modeled peak flow, and P_0 is the observed peak flow. We calculated peak flow as the average of the final six runoff rate values before rain stopped. The averaging helped to reduce error due to measurement and naturally occurring surges in runoff.

Results and Discussion

The purpose of this investigation was primarily to find whether an automated parameter estimation routine could be used with the kinematic wave–Philip infiltration model to estimate infiltration parameters. This requires showing that the model can be used with a set of physically reasonable parameters to reproduce field-measured hydrographs, that a unique "best" parameter set can be found, and further, that the parameters can be used to predict hydrographs for other antecedent conditions and plot sizes.

Most of the 92 hydrographs can be well represented with the model using physically reasonable parameters. Recall that the search space for both methods was constrained so that physically reasonable results were required. Hydraulic conductivities estimated for the road surfaces ranged from 5×10^{-5} mm/h to 8.82 mm/h with a geometric mean of 0.11 mm/h, which is reasonable for a compacted mineral soil. For comparison, *Reid and Dunne* [1984] found an average infiltration capacity of 0.5 mm/h for gravel surfaced roads on the Olympic Peninsula in Washington State. Table 3 shows statistics of errors in modeled hydrographs relative to the field-measured hydrographs, and demonstrates that errors
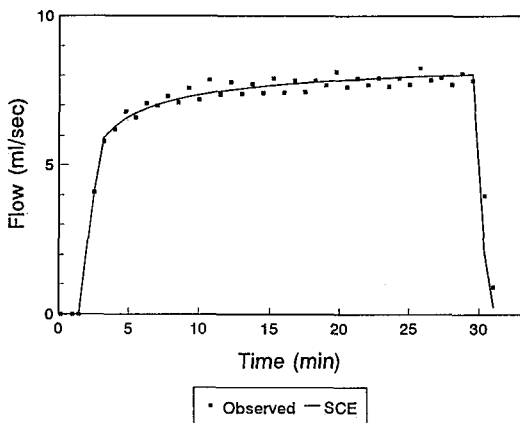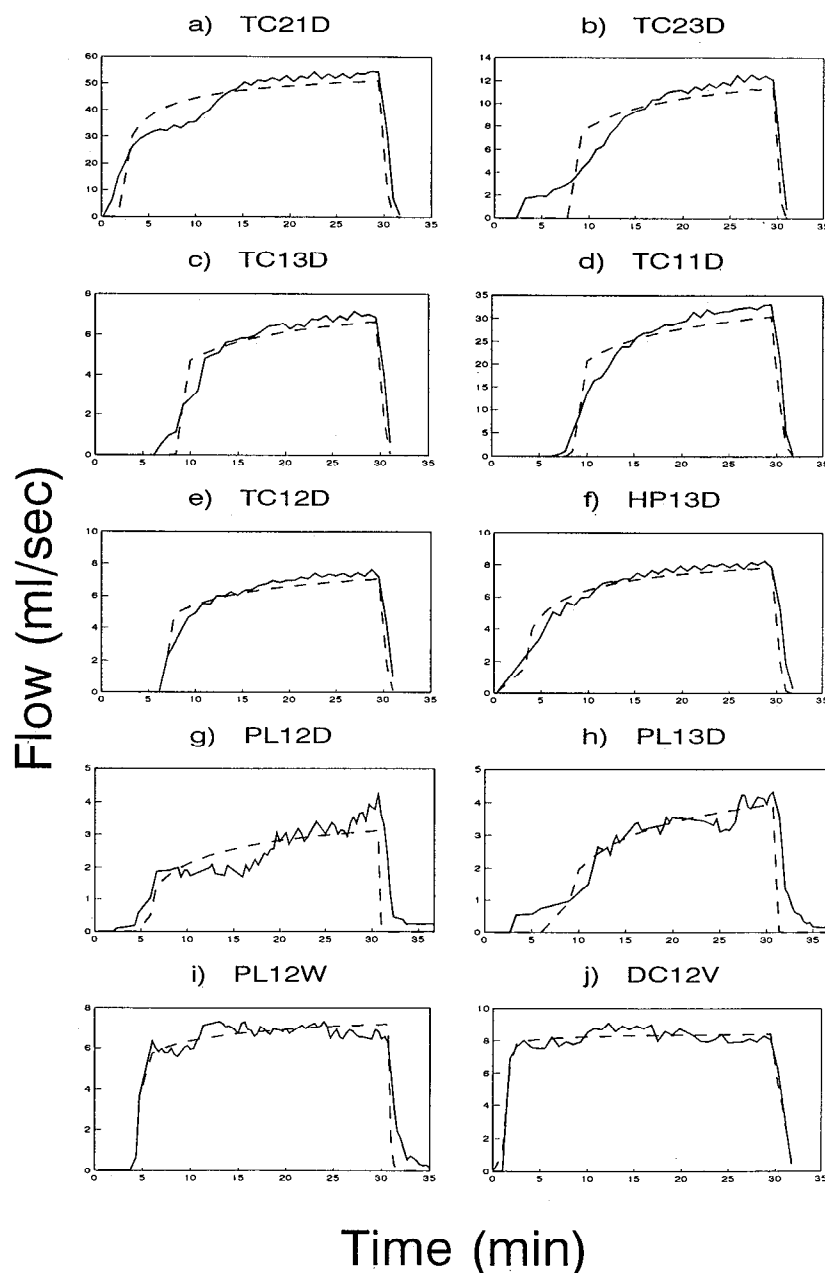
Figure 7. Ten hydrographs with the greatest errors when fitted with either algorithm. Codes above each hydrograph reflect the site in the first three digits; the fourth digit is the plot number, and the final letter reflects the dry, wet, or very wet event.

are typically small. Figure 5 shows the distribution of the absolute value of percentage error for volume and peak flow for both the Simplex and SCE methods, showing that the great majority of modeled hydrographs had less than 2% error in volume and less than 3% error in peak flow. Figure 6 shows an example of a well-represented hydrograph with volume error of 1.14% and a peak flow error of −0.51%. T tests show that the average percentage error in peak flow was essentially zero (H_0: $E_P = 0$: $p = 0.90$ for Simplex, and $p = 0.63$ for SCE), and that the percentage error in volume was consistently slightly less than zero (H_0: $E_V = 0$: $p = 2 \times 10^{-6}$ for Simplex, and $p = 7 \times 10^{-9}$ for SCE). As Table 3 demonstrates, this consistent underprediction of

volume by the estimated parameters was very small in magnitude.

Those hydrographs that were not represented well using either method typically showed either evidence of spatial variability or high variability in the runoff data. Figure 7 shows 10 of the worst hydrographs as represented by SCE estimated parameters. Figures 7a–7h were poorly represented, probably because of spatial variability in initial moisture content or depression storage. Figures 7a and 7b and 7g and 7h show a stepped shape characteristic of spatial variation, and Figures 7c–7f just show a rounding off that is not explainable except through spatial variation. All eight of these hydrographs were from the dry run of the series.
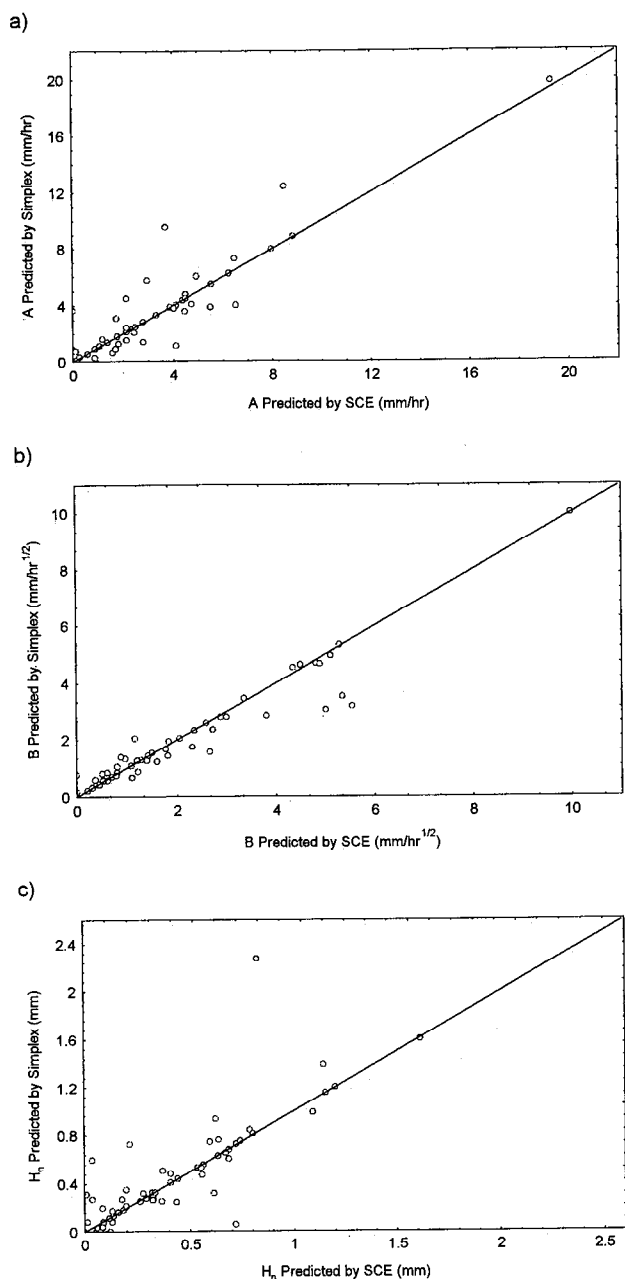
a)

b)

c)

Figure 8. Parameter values predicted by the Simplex method plotted against parameter values predicted by the SCE method with 1:1 line: (a) A, (b) B, and (c) h_n.

a) DC13V   b) TC22W

c) TC13V   d) HP11W
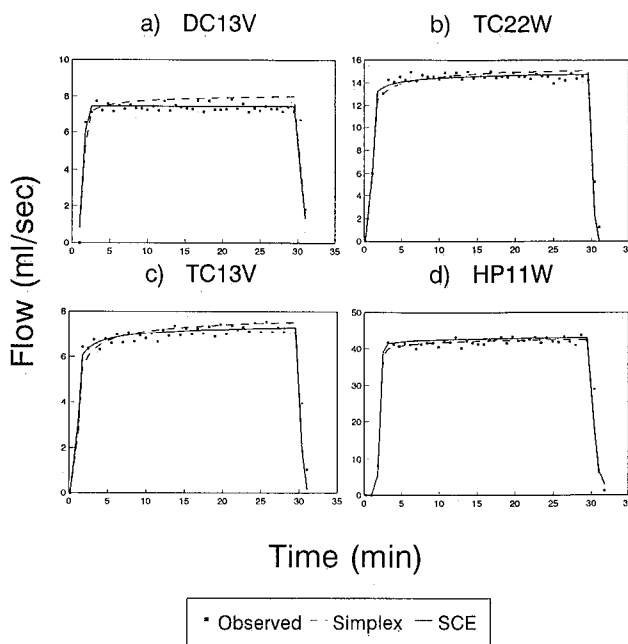

Time (min)

| • Observed - - Simplex — SCE |

Figure 9. Three hydrographs that were better fit by SCE than Simplex and one hydrograph that was better fit by Simplex than SCE.

space and raises the concern of representing hydrographs equally well with a variety of parameter sets. *Duan et al.* [1992] demonstrated the ability of the SCE approach to find the global minimum even for very flat surfaces and surfaces with many local minima, so we can accept that the parameter sets estimated by the SCE approach are very close to the "true" values. The Simplex method, however, is prone to converging in local minima and on flat surfaces. One might expect different parameter sets to result from the two different methods if the trough prevented finding unique minima. We found that the two methods converged to the same parameter values. Figure 8 shows the A, B, and h_n values for the Simplex method plotted against the A, B, and h_n for the SCE method with the 1:1 line. In paired T tests, we found that the difference between A, B, and h_n values estimated by each method did not differ significantly from zero (H_0: $A_{splx} = A_{SCE}$: $p = 0.18$, H_0: $B_{splx} = B_{SCE}$: $p = 0.12$, and H_0: $h_{n\,splx} = h_{n\,SCE}$: $p = 0.17$). The fact that both methods came to the same parameter values is strong evidence suggesting that the estimates are unique.

There were a few individual hydrographs where the SCE parameter set represented the hydrograph notably better than the Simplex parameter set (Figure 9) and one where

Subsequent events were well represented, which implies that the source of spatial variability was reduced by the first event. This could be due to moisture contents being made more uniform by the rainfall application and creation of a drainage pattern that removed dams from the microtopography of the freshly graded surface. Figures 7g and 7j show high variability in the runoff data.

The results above show that the model is capable of representing most hydrographs from forest roads well. The second issue is whether the parameter sets estimated with these automated methods are unique.

The flat trough observed in the A-B error surface in Figure 3 has an analogy in the three-dimensional A-B-h_n parameter

Table 4. Initial Moisture Content by Plot and Event for Tea Meadow

Plot	Volumetric Moisture Content			Bulk Density, g/mL
	Predry	Prewet	Pre-very Wet	
1	0.35	0.45	0.52	1.39
2	0.26	0.32	0.39	1.66
3	0.27	0.36	0.41	1.74

Table 5. Parameter Values Optimized by SCE and Hydrograph Errors for the Wet Event on the Three Plots at Tea Meadow

	Optimized Parameter Values			% Error Volume	% Error Peak Flow
Plot	A, mm/h	B, mm/h$^{1/2}$	H_n, mm		
1	2.86	1.99	2.0E−05	−0.3	−1.1
2	2.13	2.63	5.9E−02	−0.3	−2.0
3	4.75	0.65	1.3E−01	−0.7	0.5

representation by the Simplex parameter set was notably better. The differences are of the nature we saw in Figure 4 where there are tradeoffs in A and B giving similar error values. For the hydrograph in Figure 9a from Deep Creek, which went from being one of the worst representations for the Simplex method to being very well represented by the SCE method, A changed from 1.1 mm/h for the Simplex estimate to 4.1 mm/h for the SCE estimate; B went from 0.75
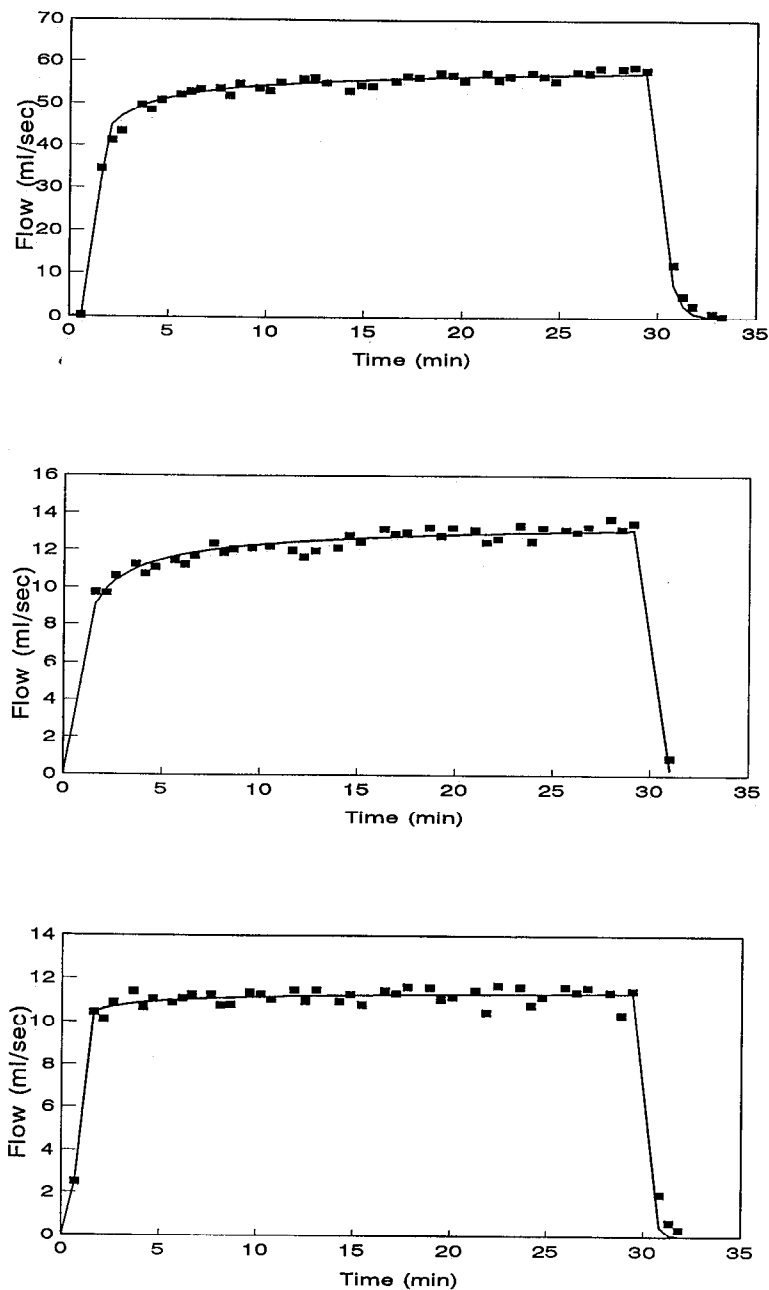

Figure 10. Actual and SCE optimized hydrographs for the wet event at Tea Meadow. (Top) Plot 1. (Middle) Plot 2. (Bottom) Plot 3.

Table 6a. Predicted Parameter Values and Hydrograph Errors Using Optimized Parameter Values From the Wet Event on Plot 1 (1 m by 5 m) at Tea Meadow

Predicted For		Predicted Parameter Values			% Error Volume	% Error Peak Flow
Plot	Event	A, mm/h	B, mm/h$^{1/2}$	H_n, mm		
1	dry	2.86	2.70	2.0E−05	5.0	0.3
1	very wet	2.86	0.00	2.0E−05	0.9	−1.7
2	dry	2.86	2.30	2.0E−05	7.5	9.7
2	wet	2.86	2.02	2.0E−05	1.4	−1.6
2	very wet	2.86	0.00	2.0E−05	0.7	0.8
3	dry	2.86	2.77	2.0E−05	−2.6	0.0
3	wet	2.86	1.63	2.0E−05	−2.1	1.5
3	very wet	2.86	0.00	2.0E−05	7.6	6.2

mm/h$^{1/2}$ to 0.16 mm/h$^{1/2}$; and h_n changed from 0.10 mm to 0.12 mm.

Showing that the model can reproduce hydrographs using physically reasonable parameters, and that a unique parameter set can be found for each hydrograph using an automated method are important steps in demonstrating that this model can be used to analyze rainfall simulation runoff data. A further question is whether the model is able to represent the changes in runoff that accompany physical changes in the soil, for example, antecedent moisture conditions. The following results from Tea Meadow suggest that the model can predict hydrographs for other antecedent conditions and plot sizes when parameters are adjusted according to physically based rules.

Table 4 presents the average soil moisture contents for several points surrounding each plot at the beginning of each event. Plot 1, the 1-m by 5-m plot, consistently showed higher moisture contents than the other two plots. The four sample locations on the fill slope side of the road (Figure 1) had high moisture contents, so the difference did not result from one spurious measurement point. This area receives less traffic and is less compacted, so the higher moisture contents are reasonable.

Table 5 shows the SCE estimated parameter set and the associated hydrograph error for the wet event on all three plots. Figure 10 graphically shows the three modeled and observed hydrographs.

Tables 6a through 6c present the adjusted parameter sets and their associated hydrograph errors for all of the combi-

nations of plots and events used. Parameters were adjusted from the estimated parameter sets in Table 5 and the moisture contents in Table 4 using (14). Note that A and h_n do not change within each table because they do not change with initial soil moisture content, but B changes by event and plot. B is zero for the very wet events, because we took the pre–very wet event soil moisture content to be the saturated soil moisture content. Tables 6a–6c are provided to show how parameters estimated from each plot performed at predicting other plots and events. The averages do differ, as shown in Table 7, but the differences between the means are not significant (H_0: $V_1 = V_2 = V_3$: $p = 0.55$ and H_0: $P_1 = P_2 = P_3$: $p = 0.68$ for peak flow).

In general, we can see that the percentage errors in volume and peak flow are small. Percentage volume errors average 2.12% and range from −6.36% to 12.34%. Percentage peak flow errors average 1.45% and range from −6.05% to 10.18%. Figure 11 shows histograms of the percentage volume and peak flow errors for the 24 cases here. Figure 12 shows predicted and observed peak flows and volumes plotted against the 1:1 line and bracketed with lines showing ±15% error.

Conclusions

The use of an automated parameter estimation algorithm with a physically based model of Horton overland flow was successful in terms of (1) reproducing field-measured hydrographs with physically reasonable parameter sets, (2) finding

Table 6b. Predicted Parameter Values and Hydrograph Errors Using Optimized Parameter Values From the Wet Event on Plot 2 (1 m by 1 m) at Tea Meadow

Predicted For		Predicted Parameter Values			% Error Volume	% Error Peak Flow
Plot	Event	A, mm/h	B, mm/h$^{1/2}$	H_n, mm		
1	dry	2.13	3.51	5.9E−02	−0.1	−1.0
1	wet	2.13	2.59	5.9E−02	−3.3	−1.5
1	very wet	2.13	0.00	5.9E−02	2.5	0.0
2	dry	2.13	2.99	5.9E−02	5.1	9.0
2	very wet	2.13	0.00	5.9E−02	2.1	2.2
3	dry	2.13	3.60	5.9E−02	−6.4	−1.2
3	wet	2.13	2.12	5.9E−02	−3.5	1.4
3	very wet	2.13	0.00	5.9E−02	9.1	7.8

Table 6c. Predicted Parameter Values and Hydrograph Errors Using Optimized Parameter Values From the Wet Event on Plot 3 (1 m by 1 m) at Tea Meadow

Predicted For		Predicted Parameter Values			% Error Volume	% Error Peak Flow
Plot	Event	A, mm/h	B, mm/h$^{1/2}$	H_n, mm		
1	dry	4.75	1.08	1.3E−01	12.3	1.7
1	wet	4.75	0.80	1.3E−01	2.8	−1.4
1	very wet	4.75	0.00	1.3E−01	−4.1	−6.1
2	dry	4.75	0.92	1.3E−01	10.9	10.2
2	wet	4.75	0.81	1.3E−01	3.6	−1.8
2	very wet	4.75	0.00	1.3E−01	−3.2	−3.1
3	dry	4.75	1.11	1.3E−01	2.6	1.5
3	very wet	4.75	0.00	1.3E−01	2.3	1.8

unique parameter sets, and (3) predicting hydrographs for other antecedent conditions and plot sizes. Eighty-four out of 92 hydrographs were described well by the model in terms of mean square error, percentage volume error, and percentage peak error, strongly suggesting that the model is appropriate to forest road surfaces. The poorly represented hydrographs may have been affected by spatial variability. The fact that both algorithms found nearly the same parameter values suggests that the error function has a unique minimum that can be found by an automated search routine. The

model predicted hydrographs for changed antecedent conditions and other plots at the same site well.

Both algorithms were able to estimate physically reasonable parameter values reliably. Given the low relief in the trough, the Simplex algorithm did better than expected. In only three out of the 84 cases that were appropriate were modeled hydrographs dramatically improved by using the parameter values estimated with SCE. These were cases where A and B tradeoffs created a sufficiently flat error surface that the Simplex method converged before finding a
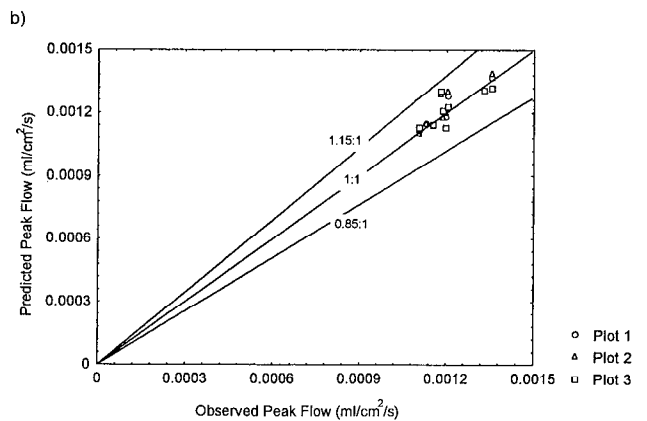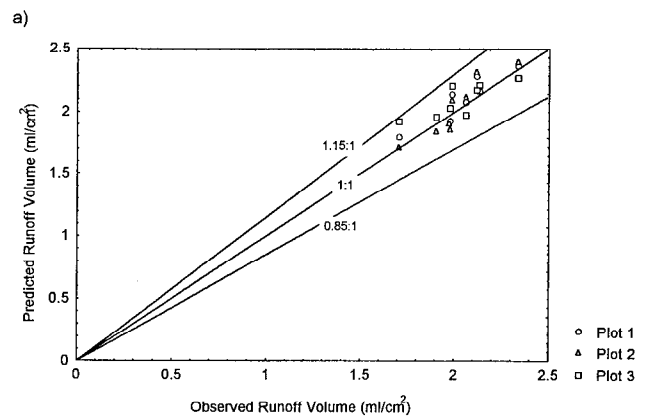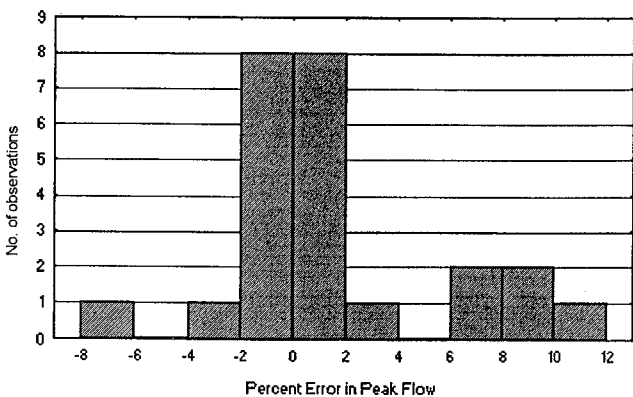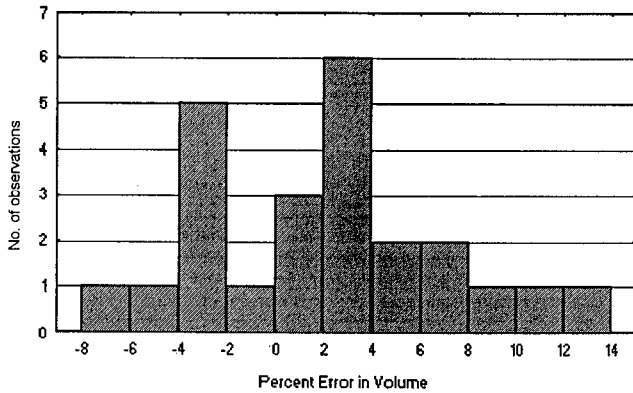

Figure 11. Distribution of percent error for predicted hydrographs at Tea Meadow.

Figure 12. Predicted versus (a) observed runoff volumes and (b) peak flows.

Table 7. Average Errors by Plot Used for Prediction

Plot	% Error Volume	% Error Peak Flow
1	2.30	1.90
2	0.68	2.09
3	3.40	0.37

global minimum. In one case, the SCE converged to a point worse than the Simplex, but the difference was small.

This demonstration that the model is capable of reproducing field-measured hydrographs with unique, physically realistic, parameter sets shows that the model is appropriate for forest roads. To further validate the model and show that this model provides a useful framework for data reduction, we demonstrated that parameter values estimated using this method can be extended to other antecedent conditions and plot sizes.

References

Burroughs, E. R., R. B. Foltz, and P. R. Robichaud, United States Forest Service research on sediment production from forest roads and timber harvest areas, paper presented at the 10th World Forestry Congress, Food and Agric. Organ., Paris, 1991.

Campbell, G. S., A simple method for determining unsaturated conductivity from moisture retention data, *Soil Sci., 117*, 311–314, 1974.

Cundy, T. W., and S. W. Tento, Solution to the kinematic wave approach to overland flow routing with rainfall excess given by Philip's equation, *Water Resour. Res., 21*(8), 1132–1140, 1985.

Duan, Q., S. Sorooshian, and V. Gupta, Effective and efficient global optimization for conceptual rainfall-runoff models, *Water Resour. Res., 28*(4), 1015–1031, 1992.

Flerchinger, G. N., and F. J. Watts, Predicting infiltration parameters for a road sediment model, *Trans. ASAE, 30*(6), 1700–1705, 1987.

Fok, Y. S., A comparison of the Green-Ampt and Philip two-term infiltration equations, *Trans. ASAE, 18*(6), 1073–1076, 1975.

Grossman, R. B., and F. B. Pringle, Describing soil surface properties—Their seasonal changes and implications for management, in Soil Survey Techniques, *Spec. Publ. 20*, pp. 57–75, Soil Sci. Soc. of Am., Madison, Wis., 1987.

Katz, D. M., The effects of surface roughness and rainfall impact on the hydraulics of overland flow, M.S. thesis, Univ. of Idaho, Moscow, 1990.

Luce, C. H., Analysis of infiltration and overland flow from small plots on forest roads, M.S. thesis, Univ. of Wash., Seattle, 1990.

Luce, C. H., and T. W. Cundy, Modifications of the kinematic wave—Philip infiltration overland flow model, *Water Resour. Res., 28*(4), 1179–1186, 1992.

Nelder, J. A., and R. Mead, A simplex method for function minimization, *Comput. J., 7*, 308–313, 1965.

Philip, J. R., Theory of infiltration, in *Advances in Hydroscience*, vol. 5, Academic, San Diego, Calif., 1969.

Philip, J. R., Inverse solution for one-dimensional infiltration, and the ratio A/K_1, *Water Resour. Res., 26*(9), 2023–2028, 1990.

Press, W. H., B. P. Flannery, S. A. Teukolsky, and W. T. Vetterling, *Numerical Recipes: The Art of Scientific Computing*, Cambridge University Press, New York, 1986.

Rawls, W. J., D. L. Brakensiek, and M. R. Savabi, Infiltration parameters for rangeland soils, *J. Range Manage., 42*(2), 139–142, 1989.

Reid, L. M., and T. Dunne, Sediment production from forest road surfaces, *Water Resour. Res., 20*(11), 1753–1761, 1984.

Ward, T. J., A study of runoff and erosion processes using large and small rainfall simulators, *Tech. Rep. 215*, N. M. Water Resour. Res. Inst., N. M. State Univ., Las Cruces, 1986.

Ward, T. J., and S. B. Bolin, A study of rainfall simulators, runoff and erosion processes, and nutrient yields on selected sites in Arizona and New Mexico, *Tech. Rep. 241*, N. M. Water Resour. Res. Inst., N. M. State Univ., Las Cruces, 1989a.

Ward, T. J., and S. B. Bolin, Determination of hydrologic parameters for selected soils in Arizona and New Mexico utilizing rainfall simulation, *Tech. Rep. 243*, N. M. Water Resour. Res. Ins., N. M. State Univ., Las Cruces, 1989b.

Ward, T. J., and S. M. Bolton, Hydrologic parameters for selected soils in Arizona and New Mexico as determined by rainfall simulation, *Tech. Rep. 259*, N. M. Water Resour. Res. Inst., N. M. State Univ., Las Cruces, 1991.

Ward, T. J., and A. D. Seiger, Adaptation and application of a surface erosion model for New Mexico forest roadways, *Tech. Rep. 188*, N. M. Water Resour. Res. Inst., N. M. State Univ., Las Cruces, 1983.

T. W. Cundy, College of Forest Resources, University of Washington, Seattle, WA 98105.

C. H. Luce, Intermountain Research Station, U.S. Department of Agriculture Forest Service, 1221 South Main, Moscow, ID 83843.